Early stages of spinodal decomposition in Fe–Cr resolved by in-situ small-angle neutron scattering

M. Hörnqvist,[1, a)] M. Thuvander,[1] A. Steuwer,[2, 3] S. King,[4] J. Odqvist,[5] and P. Hedström[5]
[1)] *Applied Physics, Chalmers University of Technology, Fysikgränd 3, S-412 96, Gothenburg, Sweden*
[2)] *MAX IV Laboratory, Lund University, S-221 00, Lund, Sweden*
[3)] *Nelson Mandela Metropolitan University, Gardham Av., Port Elizabeth 6031, South Africa*
[4)] *ISIS Facility, Rutherford Appleton Laboratory, Chilton, OX11 0QX Didcot, United Kingdom*
[5)] *Materials Science and Engineering, KTH Royal Institute of Technology, Brinellvägen 23, S-100 44, Stockholm, Sweden*

(Dated: 3 March 2017)

In-situ, time-resolved small-angle neutron scattering (SANS) investigations of the early stages of the spinodal decomposition process in Fe–35Cr were performed at 773 and 798 K. This is the first time in-situ SANS has been used to study the short-term structure evolution in the Fe–Cr system. The kinetics of the decomposition, both in terms of characteristic distance and peak intensity followed a power-law behaviour from the start of the heat treatment (a'=0.10–0.11 and a''=0.67–0.86). Furthermore the method allows tracking of the high–Q slope, which is a sensitive measure of the early stages of decomposition. Ex-situ SANS and atom probe tomography was used to verify the results from the in-situ investigations. Finally, the in-situ measurement of the evolution of the characteristic distance at 773 K was compared with predictions from the Cahn-Hilliard-Cook model, which showed good agreement with the experimental data (a'=0.12–0.20 depending on the assumed mobility).

Spinodal decomposition of the bcc phase in Fe–Cr alloys into an Fe-rich and a Cr-rich phase is a widely studied phenomenon. The reason is two-fold: Firstly, the system is the basis of the industrially important stainless steel family, where the decomposition of the bcc phase in ferritic, duplex and to some extent martensitic and δ-ferrite containing austenitic grades, is partially responsible for degradation of the mechanical properties over time during elevated temperature exposure in service. Secondly, the Fe–Cr system is ideal to study the fundamentals of the spinodal decomposition process, since it offers a combination of a wide miscibility gap, a rather wide temperature range where the kinetics of the decomposition is suitable for practical measurements, and minor coherency strains. The decomposition process in Fe–Cr is typically investigated by transmission electron microscopy (TEM)[1], Mössbauer spectroscopy[2,3], atom probe tomography (APT)[4,5] or small-angle neutron scattering (SANS)[6–8]. While each technique has its specific advantages, only SANS readily offers the possibility to perform time-resolved in-situ measurements at elevated temperatures. However, so far only very few investigations have taken advantage of this possibility of direct continuous tracking of the kinetics without any specimen-to-specimen variations in composition, starting structure or isothermal temperature. For the Fe–Cr(–Ni) system, there are only two readily available reports of in-situ SANS experiments[9,10], although other systems have been investigated more recently, e.g. Fe–Co–Mo[11]. In[9,10], acquisition times of several hours were used, which resulted in poor temporal resolution. Furusaka et al.[12] used in-situ SANS to investigate the critical scattering of Fe–Cr alloys in the vicinity of the Curie temperature, but the subsequent investigations of aged alloys were performed ex-situ.

The existence and location of the spinodal in the binary Fe–Cr system is today well described, both from thermodynamic modelling and experiments (see e.g. reference[13] and references therein). Direct observations using three dimensional APT investigations have also demonstrated the transition from phase separation through nucleation-and-growth to spinodal decomposition in the composition range 25 to 35 % Cr[13]. Whereas the spinodal nature of the decomposition process have been questioned for similar systems, e.g. Fe–Cr–Co[14], based on the development of the SANS invariant during ageing, similar studies of the Fe–Cr binary system show no such indications[6]. During the spinodal decomposition a characteristic interconnected structure with nano-scale modulations of the composition forms. This results in the appearance of an interference peak in the structure factor at scattering vector Q_p ($Q = 4\pi \sin\theta/\lambda$, where λ is the neutron wavelength and θ is half the scattering angle) corresponding to a characteristic length scale $\Lambda = 2\pi/Q_p$, usually interpreted as the modulation wavelength of the decomposed α-α' structure. Typically, Q_p follows a power-law relationship with annealing time, $Q_p \propto t^{-a'}$. Similarly, the maximum scattered intensity follows $I_p = \mathrm{d}\Sigma/\mathrm{d}\Omega(Q_p) \propto t^{a''}$, where $\mathrm{d}\Sigma/\mathrm{d}\Omega$ is the macroscopic scattering cross-section (from hereon, I is used instead of $\mathrm{d}\Sigma/\mathrm{d}\Omega$ for brevity). Such behaviour

[a)] magnus.hornqvist@chalmers.se

is in general agreement with both theoretical predictions (where a'=1/6 and a''=1/2)[15] and Monte-Carlo simulations (yielding a'=0.2–0.28 and a''=0.65–0.74)[16,17].

In the present letter we present the first time-resolved in-situ SANS investigation of spinodal decomposition in the Fe–Cr system with sufficient temporal resolution to study the early stages of the process. The aim is to investigate the short-time kinetics of spinodal decomposition in the relevant stages where embrittlement often occurs[18]. Furthermore, the in-situ data are used to make comparisons with theoretical predictions from the Cahn-Hilliard-Cook (CHC) model[7,19].

The binary Fe–Cr alloy was produced by vacuum arc melting (see[13] for more details on material preparation), followed by solution treatment at 1373 K for 2 h under pure argon, and a final quench in brine. The final alloy composition (in wt.-%) was Fe–36.1Cr–0.27Si–0.09Mn–0.02Ni–0.008N–0.005P–0.005C. This composition is within the spinodal, and has been shown previously to results in the characteristic interconnected structure during ageing at the intended temperatures[13]. The material was cut into approximately 1.5 mm thick pieces with a 10×10 mm square cross-section and subsequently ground and polished to remove surface oxides.

SANS data were obtained on the LOQ small-angle diffractometer at the ISIS Pulsed Neutron Source (STFC Rutherford Appleton Laboratory, Didcot, U.K.)[20]. This is a fixed-geometry white beam time-of-flight instrument which utilizes neutrons with wavelengths between 0.2 and 1.0 nm. Data are simultaneously recorded on two, two-dimensional, position-sensitive neutron detectors, to provide a simultaneous Q-range of 0.06–14 nm^{-1}.

A vacuum furnace was used to heat the specimens during in-situ measurements. The specimens were mounted in pockets made from vanadium sheet (with negligible coherent scattering cross-section), and a thermocouple was placed close to the specimen to monitor and control the temperature. During the tests, the specimens were heated as rapidly as possible without causing temperature over-shoots, giving typical heat-up times of around 20 minutes, and the measurements were started immediately upon reaching the desired temperature (773 and 798 K). Measurements lasting 15 minutes were performed back-to-back for a total time of 10 h, i.e. each data set consisted of data time-averaged over 15 min.

The raw scattering data was corrected for detector efficiencies, sample transmission and background scattering (including contribution from the Vanadium pocket) and converted to macroscopic scattering cross-section using the MantidPlot software[21], version 3.1.1. The data were placed on an absolute scale (cm^{-1}) using the scattering from a standard sample (a solid blend of hydrogenous and perdeuterated polystyrene) in accordance with established procedures[22]. In the present investigation, no external magnetic field was applied due the configuration of the furnace. The recorded scattering is the sum of the nuclear and magnetic contributions, where the latter is related to both magnetic domain structure and spin-misalignment, see e.g.[23]. This can be problematic, since the structure factors for nuclear and magnetic scattering are not necessarily the same, and the length scales can overlap. Previous studies have used argued that the nuclear and magnetic contributions are proportional, based on separation of the cross-sections in an applied magnetic field. This does not ensure proportionality in the absence of magnetic saturation, since the applied magnetic field removes the domain structure and spin-misalignment present in its absence. However, Isalgué et al.[24] showed that the structure factor of a decomposed Fe–28Cr–2Mo–4Ni–Nb alloy obtained with and without an applied magnetic field (5 kOe) were proportional above $Q > 0.5$ nm^{-1}. The increased scattering lower Q in the absence of an applied magnetic field was attributed to the presence of magnetic domains. Since the length scale of the domain structure is much larger that the expected modulation wavelength of the decomposed structure, it should not interfere with the present measurements. As the magnetic field is expected to remove, or at least significantly reduce the contribution also from spin-misalignment, the measured proportionality between scattering with and without external magnetisation, suggest that also the contribution from spin-misalignment is negligible. Note that this only applies to the measurement of the peak position, Q_p, and not to the scattered intensity, which can be several orders of magnitude larger for the spin-alignment than for the nuclear contribution[23]. Although the study by Isalgué et al.[24] was performed at room temperature, the good agreement between in-situ and ex-situ data obtained herein, suggests that the assumption holds also at elevated temperatures. Furthermore, the results are validated against APT data, which are independent of the distribution of magnetic moments.

In order to separate the scattering contribution from the spinodal decomposition process, the following procedure was applied to each data set. A polynomial was fitted to the $\log(I)$ vs. $\log(Q)$ curve, excluding the region where scattering from the decomposition process was observed, in order to separate the background signal (I_b). Whereas ideally the scattering curve obtained directly after heating would be used to define the background, the procedure above was necessary since the background was not constant during the experiments. By dividing the scattered signal by the background, a normalised signal ($I_n = I/I_b$) was obtained. This normalised signal was fitted with a Gaussian function, I_{nG}, with $\log(Q)$ as argument, and the signal from the spinodal decomposition was calculated as $I_{sd} = I_b(I_{nG} - 1)$. The procedure is outlined graphically in Fig. 1. The reason for using a Gaussian fit of I_n rather than just subtracting the fitted background from the total signal was two-fold. Firstly, using the normalised signal proved to be more sensitive in the early stages of the separation. Secondly, the procedure ensures that there are no spurious negative data points arising from the subtraction. The values of interest, Q_p and I_p, was then extracted from the obtained

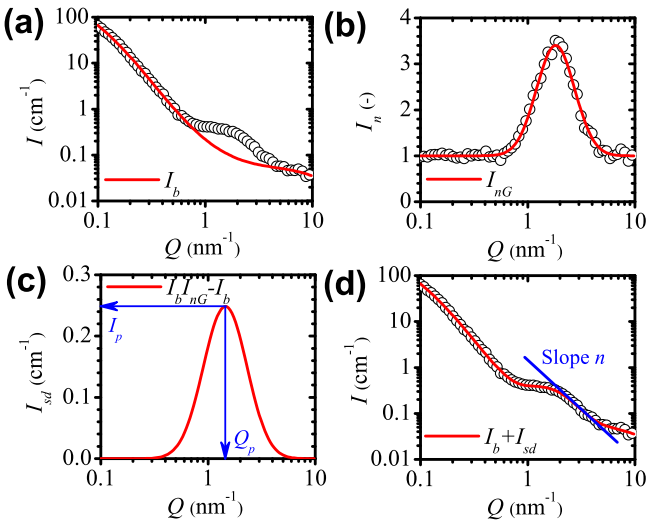

FIG. 1. (a) Fitting of background, I_b. (b) Fitting of a Gaussian function, I_{nG}, to the normalised signal, $I_n = I/I_b$. (c) Calculation of scattered signal from spinodal decomposition, $I_{sd} = I_b(I_{nG} - 1)$. Arrows show the identification of Q_p and I_p. (d) Total signal, $I = I_b + I_{sd}$, including an illustration of the high–Q slope, n.

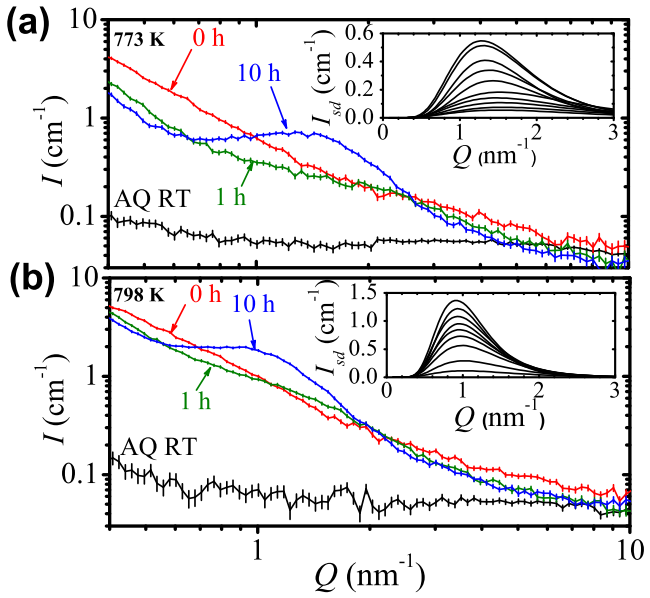

FIG. 2. In-situ scattering curves obtained before ageing (AQ RT), directly after heating (0 h) and after 1 and 10 h ageing at (a) 773 and (b) 798 K. The inserts show the scattering from the spinodal decomposition, I_{sd} , for selected ageing times.

Q–I_{sd} curves, as shown in Fig. 1(c).

For comparison, two quenched specimens were also subjected to ex-situ heat treatments at 773 K for 1 and 10 h, and investigated by ex-situ SANS at room temperature, employing otherwise the same experimental settings (apart from exposure time) and evaluation procedure as described above. The experimental data was also compared with theoretically predicted structure factor, $S(Q,t)$ from the CHC equation[7,19]

$$S(Q,t) = \frac{RT}{f'' + 2\kappa Q^2} + \left[S_0 - \frac{RT}{f'' + 2\kappa Q^2}\right] \times \exp\left\{-2M(f'' + 2\kappa Q^2)Q^2 t\right\} \quad (1)$$

where $S_0 = S(Q, t = 0)$ is the structure factor of the as-quenched material, f'' is the second derivative of the free energy with respect to composition, κ is the gradient energy coefficient and M is the atomic mobility. Following Marro and Vallés[25], $S_0 = 1 - x_0^2$, where x_0 is the average Cr content. The peak in the calculated structure factor was evaluated at 773 K for times ranging from 15 min up to 10 h. At 798 K the predicted second derivative of the molar Gibbs free energy with respect to the mole fraction of Cr is positive i.e. outside the spinodal, and therefore only calculations at 773 K was performed.

Figure 2 shows the scattering curves obtained directly after reaching the ageing temperature (0 h), as well as after 1 h and after 10 h of ageing at 773 or 798 K. Also included is the as-quenched data recorded at room temperature before heating (AQ RT). The error bars show the statistical error associated with the data acquisition. The increased background at elevated temperatures has been attributed to critical magnetic scattering in the vicinity of the Curie temperature[10]. From Fig. 2 it is clear why the 0 h curve could not be subtracted as background, as the magnitude of the scattering is significantly higher over the entire Q-range compared to the background in other data sets. The reason for the large difference between curves at 0 h and the subsequent acquired data sets is not clear at present. This deviation, as well as the reason for the slowly shifting background, should be further investigated in order to provide a better procedure for background subtraction. Based on the procedure outlined above, the scattering from the spinodal decomposition is shown for selected times in the inserts in Fig. 2.

Figure 3 shows the development of the characteristic distance and peak height with ageing time. Both Λ and I_p clearly follows the expected power-law behaviour, with a'=0.10 and 0.11, and a''=0.67and 0.86, at 773 and 798 K, respectively. The error bars in Fig. 3(a) represent the estimated drift in the peak position from the temporal averaging over 15 min, and is based on the local derivative of the power law fits ($\epsilon_i = \pm\dot{\Lambda}_i \Delta t$, where ϵ_i is the error in data point i, $\dot{\Lambda}_i$ is the derivative of Λ with respect to time at time t_i and Δt is half the measurement time). This error was found to dominate over the uncertainty in the process of determining Q_p. In Fig. 3(b) the error is based on estimated uncertainty from the fitting of I_b.

The in-situ data agrees well with the results from ex-situ tests of specimens annealed at 773 K. The absolute magnitudes of both Λ and I_p are consistently slightly higher in the in-situ experiments, compared to the tests performed ex-situ. This could possibly be a result of the background subtraction process, since the shape of

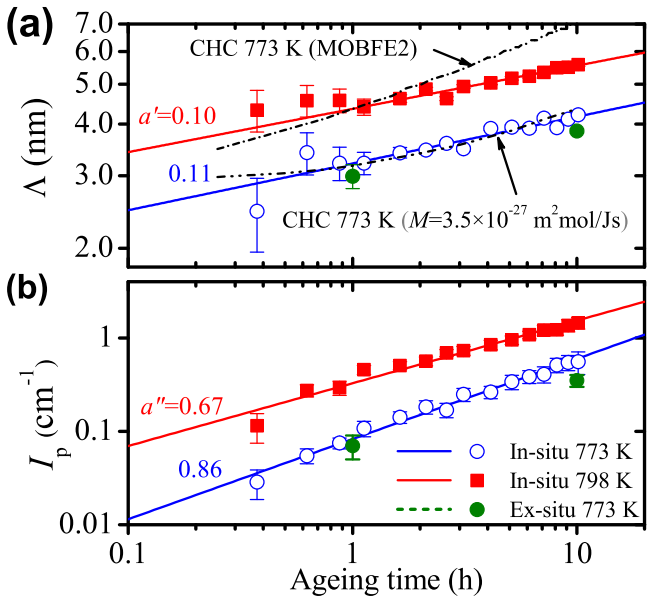

FIG. 3. Time evolution of (a) characteristic distance ($\Lambda = 2\pi/Q_p$) and (b) maximum scattered intensity from the spinodal decomposition ($I_p = \mathrm{d}\Sigma/\mathrm{d}\Omega(Q_p)$). The black lines show the results from the Cahn-Hilliard-Cook model at 773 K using either mobilities from the *MOBFE2* database, or a constant mobility $M = 3.5 \times 10^{-27}$ m^{2}mol×J^{-1}s^{-1}.

the Q-dependent background is different at ambient and elevated temperatures, or more likely because the temperatures were not identical during in-situ and ex-situ ageing. Comparing the 773 and 798 K data, the differences in both peak position and magnitude are much larger than between the in-situ and ex-situ results. Given that a temperature difference of 25 K have such a large effect, it could be expected that even a small difference in ageing temperature can have an observable impact. This further emphasises the advantage of in-situ measurements in order to establish reliable kinetic data, and points to the need of more precise thermometry in both in-situ and ex-situ ageing if values from different tests are to be compared. The value of Λ after 10 h ageing at 773 K also agrees well with the reported modulation wavelength measured by APT[5], see Table I.

The obtained exponents (a'=0.10–0.11, a''=0.67–0.86) are in the same range as the available literature data[6–8,10,12,26], although a' is slightly smaller than usually observed. This may be related to the early stages of decomposition studied, since the data presented in e.g.[8] shows that the slope is smaller at short ageing times (less than 10 h and 1 h at 773 and 798 K, respectively). It is also highly interesting to compare the in-situ data with the CHC theory of spinodal decomposition. The results from the model with $f'' = -261$J×mol^{-1}, $\kappa = 4.07 \times 10^{-16}$ J×m^{-2}mol^{-1}, and the mobility calculated from the *MOBFE2* database ($M = x_0(1-x_0)(x_0 M_{\mathrm{Fe}} + [1-x_0]M_{\mathrm{Cr}}) = 3.49 \times 10^{-26}$ m^{2}mol×J^{-1}s^{-1}, with $M_{\mathrm{Fe}} = 6.4 \times 10^{-26}$ and $M_{\mathrm{Cr}} = 2 \times 10^{-25}$ m^{2}mol×J^{-1}s^{-1}) are included in Fig. 3. The theoretical predictions have a similar behaviour to the experimental data, but the absolute magnitude of Λ is too high, and $a' = 0.20$ is higher than experimentally observed. This disagreement is not unexpected since the mobilities are highly uncertain at 773 K due to the large extrapolations from higher temperatures. By assuming a lower mobility (in our case $M = 3.5 \times 10^{-27}$ m^{2}mol×J^{-1}s^{-1}), good agreement between the CHC predictions and the experimental data is obtained ($a' = 0.12$ and similar magnitudes). This is consistent with previous phase-field simulations of spinodal decomposition in Fe–Cr[27], where the predicted kinetics based on exitting thermodynamic databases were too fast compared to experiments. It could be noted that the CHC predictions also show a gradually increasing slope with ageing time in the early stages, in agreement with the results in[8]. As the theoretical model only describes the structure factor due to composition modulations, and does not consider any magnetic contributions, the agreement could be taken as further support for the negligible effect of magnetic scattering in the present case.

TABLE I. Comparison of the characteristic distance (in nm) after ageing at 773 K obtained from in-situ and ex-situ SANS (present investigation), and modulation wavelength from RDF analysis of APT data[5].

Time	In-situ	Ex-situ	APT
1 h	3.2	3.0	–
10 h	4.2	3.9	3.8

Another characteristic feature associated with the progressing decomposition is the slope, n, of the $\log(I)$ vs. $\log(Q)$ curve beyond Q_p (see Fig. 1(d)). A value of $n = 4$ (Porod's law) indicates sharp interfaces, whereas $n = 2$ is indicative of diffuse compositional fluctuations. In the case of spinodal decomposition, $n = 4$ is usually taken as an indication of a fully developed structure in the coarsening stage. The slope has been used by e.g. Ujihara

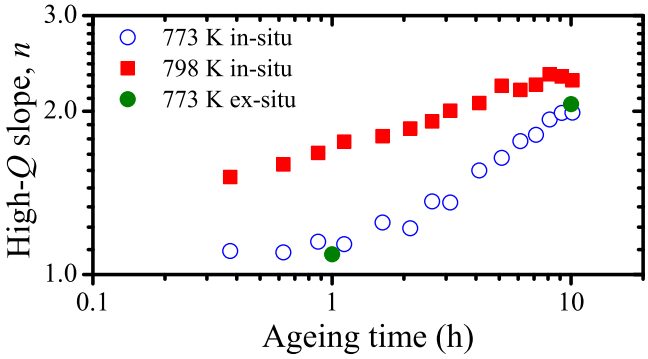

FIG. 4. Change in n, the slope of $\log(I)$ vs. $\log(Q)$ on the high-Q side of the interference peak, with ageing time.

and Osamura[8] and Furusaka et al.[28] as a means to characterise the development of the decomposition. Figure 4 shows the development of n with ageing time, where an approximate power-law behaviour is observed. During the in-situ tests, n increases from around 1 to approximately 2 at 773 K, and from 1.5 to slightly below 2.5 at 798 K. The results are consistent with those from the ex-situ measurements, and indicate that the structure is in the early stages of development after 10 h at the current test temperatures.

Although the present results have been obtained with much higher temporal resolution than previously published for the Fe–Cr system, further use of high-flux instruments will enable measurements that can reveal unprecedented details of the early stages of the decomposition. In addition, clarification of the origin of the time-dependent background is necessary in order to improve the procedure for background subtraction. Although the good agreement between the results from the in-situ experiments and APT, as well as with theory, suggest that contributions from spin-alignment is negligible in the present case, further studies on the effect of external magnetisation on the scattering behaviour are necessary to verify this.

In summary, the results presented here represent the first in-situ investigation of the early stages of spinodal decomposition in the Fe–Cr system. The results show that both the characteristic distance and intensity at 773 and 798 K follow a power-law behaviour, and the evolution at 773 K is in good agreement with theoretical predictions from the Cahn-Hilliard-Cook model with constant mobility. Furthermore the method allows tracking of the high–Q slope, which is a sensitive measure of the early stages of decomposition.

This work was supported by the HERO-M (Hierarchical Engineering of Industrial Materials) Centre at the Royal Institute of Technology and the Carl Tryggers Foundation. The access to the LOQ beam line at ISIS was provided through grant number RB 1320394. Mr. Paul McIntyre at ISIS is kindly acknowledged for invaluable assistance with the in-situ furnace, and Mr. Xin Xu at KTH is acknowledged for sample preparation.

[1] P. Hedström, S. Baghsheikhi, P. Liu, and J. Odqvist, Mater. Sci. Eng. A **534**, 552 (2012).
[2] D. Chandra and L. Schwartz, Metall. Trans. **2**, 511 (1971).
[3] J. Cislak, S. Dubiel, and B. Sepiol, J. Phys.: Condens. Matter **12**, 6709 (2000).
[4] M. Miller, J. Hyde, M. Hetherington, A. Cerezo, G. Smith, and C. Elliott, Acta Metall. Mater. **9**, 3385 (1995).
[5] J. Zhou, J. Odqvist, M. Thuvander, and P. Hedström, Microsc. Microanal. **19**, 665 (2013).
[6] F. Bley, Acta Metall. Mater. **40**, 1505 (1992).
[7] J. LaSalle and L. Schwartz, Acta Metall. **34**, 989 (1986).
[8] T. Ujihara and K. Osamura, Acta Mater. **48**, 1629 (2000).
[9] K. Hawick, J. Epperson, C. Windsor, and V. Rainey, in *Materials Research Society Meeting. Symposium F.* (MRS, 1990).
[10] J. Epperson, V. Rainey, C. Windsor, K. Hawick, and H. Chen, in *Materials Research Society Meeting. Symposium F.* (MRS, 1990).
[11] E. Eidenberger, M. Schober, P. Staron, D. Caliskanoglu, H. Leitner, and H. Clemens, Intermetallics **18**, 2128 (2010).
[12] M. Furusaka, Y. Ishikawa, S. Yamaguchi, and Y. Fujino, J. Phys. Soc. Japan **55**, 2253 (1986).
[13] W. Xiong, P. Hedström, M. Selleby, J. Odqvist, M. Thuvander, and Q. Chen, CALPHAD **35**, 355 (2011).
[14] Y. Wang, R. Kampmann, and R. Wagner, Physica B **234-236**, 992 (1997).
[15] K. Binder and D. Stauffer, Phys. Rev. Lett. **33**, 1006 (1974).
[16] J. Marro, A. Bortz, M. Kalos, and J. Lebowitz, Phys. Rev. B **12**, 2000 (1975).
[17] J. Marro, J. Lebowitz, and M. Kalos, Phys. Rev. Lett. **43**, 282 (1979).
[18] P. Hedström, F. Huyan, J. Zhou, S. Wessman, M. Thuvander, and J. Odqvist, Mater. Sci. Eng. A **574**, 123 (2013).
[19] H. Cook, Acta Metall. **18**, 297 (1970).
[20] R. Heenan, J. Penfold, and S. King, J. Appl. Cryst. **30**, 1140 (1997).
[21] `http://www.mantidproject.org`, home of the Mantid project, with information, documentation and software download.
[22] G. D. Wignal and F. S. Bates, J. Appl. Cryst. **20**, 28 (1987).
[23] A. Michels and Weissmüller, Rep. Prog. Phys. **71**, 066501 (2008).
[24] A. Isalgué, M. Anglada, J. Rodriquez-Carvajal, and A. de Geyer, J. Mater. Sci. **25**, 4977 (1990).
[25] J. Marro and J. Valles, Phys. Letters **95A**, 443 (1983).
[26] S. Katano and M. Iizumi, Physica B **120**, 392 (1983).
[27] W. Xiong, M. Selleby, Q. Chen, J. Odqvist, and Y. Du, Crit. Rev. Sol. State Mater. Sci. **35**, 125 (2010).
[28] M. Furusaka, Y. Ishikawa, and M. Mera, Phys. Rev. Lett. **54**, 2611 (1985).